


Memory effect and phase transition in a hierarchical trap model for spin glasses

Depei Zhang, Tianran Chen, Marija Vucelja, Seung-Hun Lee, and Gia-Wei Chern
Department of Physics, University of Virginia, Charlottesville, Virginia 22904, USA

 (Received 14 August 2018; accepted 18 November 2021; published 6 December 2021)

We introduce an efficient dynamical tree method that enables us to explicitly demonstrate the thermoremanent magnetization memory effect in a hierarchical energy landscape. Our simulation nicely reproduces the nontrivial waiting-time and waiting-temperature dependences in this nonequilibrium phenomenon. We further investigate the condensation effect, in which a small set of microstates dominates the thermodynamic behavior in the multilayer trap model. Importantly, a structural phase transition of the multilayer tree model is shown to coincide with the onset of the condensation phenomenon. Our results underscore the importance of hierarchical structure and demonstrate the intimate relation between the glassy behavior and structure of barrier trees.

DOI: [10.1103/PhysRevE.104.064105](https://doi.org/10.1103/PhysRevE.104.064105)

I. INTRODUCTION

Understanding the nature of spin-glass dynamics remains a challenging task in modern statistical and condensed matter physics. The glass phase is intrinsically nonstationary: A glass system in the thermodynamic limit continues to relax toward its ground state with an ever slower rate. A hallmark of spin glasses at low temperatures is the aging phenomena, which originate from a history-dependent relaxation dynamics of these systems [1–4]. One particularly intriguing dynamical behavior related to aging is the memory effect [5]. For example, in the so-called zero-field-cooled (ZFC) aging experiments [6–8], a spin glass is quenched below its freezing temperature in the absence of magnetic field. After a waiting time t_w , an external magnetic field is turned on and the resultant magnetization M often depends on the duration of the waiting period. Various experimental setups with different cooling and heating protocols have been employed to investigate the memory effect of glassy systems [9–19].

The memory effect is intimately related to the rejuvenation phenomena, which are manifestations of the extreme sensitivity of spin-glass systems to temperature changes [11–14]. Specifically, for example, when a spin glass is subject to a small negative temperature jump in the glass phase, the system behaves as if it had been quenched from above the glass transition temperature T_f . However, a perfect memory of the time spent at the initial temperature below T_f is somehow kept, as demonstrated by the so-called memory-dip experiments [13–19]. These intriguing nonequilibrium behaviors are believed to be related to a certain “coherence” length that keeps on growing in an aging spin glass [20–24]. The relaxation dynamics in the glass phase is thus characterized by multiple timescales that govern the dynamics of the spin glass at different length scales. This dynamic temperature-chaos picture that involves multiple timescales and length scales is supported by numerical simulations based on the real-space droplet models [25–27] and recent large-scale Monte Carlo simulations of three-dimensional Edwards-Anderson spin-glass models [28].

While valuable insights and intuition about the aging dynamics can be gained from the real-space approaches [22–24,28–33], the multiscale nature of the memory and rejuvenation phenomena makes such direct simulations computationally very difficult, if not impossible. On the other hand, theoretical approaches based on the state-space or energy landscape methods have long been successfully applied to quantitatively model the aging phenomena in glass systems. This is because multiple energy scales and timescales can be easily encoded into dynamical models based on energy landscapes [34–51]. A canonical example is the random energy model [34,35], in which the lifetime of the many metastable states of the glass system is assumed to be a random variable described by a broad power-law distribution. The aging phenomenon in such models can be attributed to a divergent relaxation time when averaged over all the local minimum states.

Various studies have emphasized the hierarchical structure of the energy landscape for spin glasses [41–45,52–55]. A diffusion process in such hierarchical structures can naturally lead to nontrivial relaxational dynamics such as stretched exponential decay or power-law decay with a temperature-dependent exponent [41–43]. Moreover, the hierarchical diffusion problem can be mapped into a random-walk problem on a tree structure, with its nodes corresponding to the many metastable states of the energy surface. Highly nontrivial glassy phenomena can be quantitatively reproduced by such tree models coupled with a master-equation approach. For example, the magnetization response observed in the standard ZFC experiments can be nicely reproduced by the binary tree models [42–44]. Nonequilibrium dynamical responses, such as the ac susceptibility memory effect, can be described by the tree models with random-walk dynamics [46–48]. In addition to phenomenological hierarchical tree models, a quantitative barrier tree representation of specific spin models can also be realized based on the concept of disconnectivity graphs [56–64].

In this paper we develop a hierarchical tree model and apply it to simulate the thermoremanent magnetization (TRM) memory-dip phenomena observed in several spin glasses [12–19]. In such experiments, the sample is first cooled down from well above T_f to a base temperature with a single stop for a waiting time t_w at an intermediate temperature T_w in zero magnetic field. Once at the base temperature, the system is heated back to high temperature and its magnetization M is measured with a small probing field. The waiting period allows the system to evolve toward equilibrium at the temperature T_w . Interestingly, the quasiequilibrium established during the stop seems to be kept in memory, and the dc magnetic susceptibility exhibits a remarkable dip at T_w when heated back. Our random-walk simulations on the proposed dynamical tree model capture essential features of the TRM memory effect, particularly the nontrivial waiting-time and waiting-temperature dependences of the susceptibility dip.

We further show that the magnitude of the memory effect depends crucially on the structure of the hierarchical tree, which is quantitatively characterized by a parameter λ . Essentially, this parameter controls the branching probability of the backbone tree, which consists only of saddle points. In the tree representation, a node with large branching indicates a larger configuration entropy associated with this saddle point. In order to efficiently model the effect of large branching, a dynamical tree method where the relevant nodes are generated on the fly is introduced. We find that the hierarchical tree of the energy landscape exhibits a structural phase transition at a critical λ_c above which glassy behaviors disappear. This critical point is further associated with the condensation phenomenon that results from a competition between energy and entropy.

The rest of the paper is organized as follows. In Sec. II we review the basics of the barrier tree representation of the hierarchical energy landscape. We next discuss the dynamical tree method and the random-walk simulations for simulating the TRM memory-dip experiments. The effect of the tree structure on the memory effect is further explored in Sec. III. We show that a structural transition of the tree at $\lambda_c = 1$ coincides with the condensation transition, which plays an important role in the nonequilibrium behaviors of the glassy systems. We provide a summary in Sec. IV.

II. DYNAMICAL HIERARCHICAL TREE MODEL FOR THE MEMORY EFFECT

We begin with a discussion of the tree representation of the hierarchical energy landscape [41,60]. Two examples of the barrier trees are shown in Fig. 1. Each node of the tree, denoted by a circle, represent either a saddle point or a local energy minimum. The closed and open red circles correspond to boundary and internal saddle points, respectively, of the energy landscape. Each line emanating from a circle represents a downward path from the saddle point of the energy landscape. These lines could end at another saddle point at a lower energy or at a local minimum. For simplicity, both types of nodes descended from a saddle point are called the daughters of the saddle node. A boundary saddle point (closed red circle) only has local minima as its daughters, while an internal saddle (open red circle) could also have other saddle nodes at a

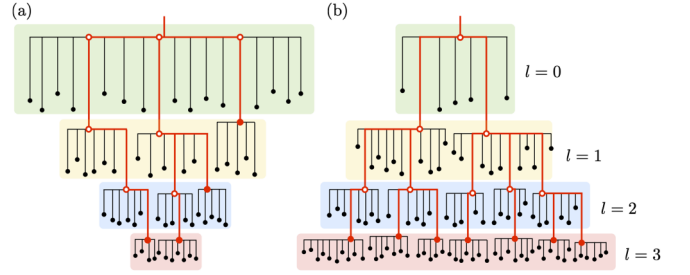


FIG. 1. Schematic diagram of hierarchical barrier trees with (a) $\lambda = 0.5$ and (b) $\lambda = 2.0$. Each node, represented by a circle, of the tree corresponds to either a saddle point or a local minimum. Red closed (open) circles denote the boundary (internal) saddle points, while black circles represent local minima. The backbone of the tree is highlighted by red lines, which also show the connectivity of the saddle points. Note that the level index l increases from top to bottom.

lower level as its daughter. Each local minimum node (black circles in Fig. 1) in the tree represents a phase-space pocket in which the system can be trapped. The edge between two nodes indicates a possible dynamical pathway; the corresponding barrier height is indicated by the edge length. Finally, a level index l is introduced to count the distance, or the number of branching, of a node from the root.

The barrier energy ε_l of local minima at the l th level or that of saddle points at the $(l + 1)$ th level is a random number drawn from an exponential distribution

$$\rho_l(\varepsilon_l) = e^{-\varepsilon_l/T_l}/T_l. \quad (1)$$

Importantly, this probability density gives rise to a divergent trapping time for minima at level l when the temperature $T < T_l$. In order to compute the magnetic susceptibility χ , a magnetization parameter m_l is assigned to each node following the random magnetization model [46–48], where m_l is a random number uniformly distributed in the interval $[-\mathcal{M}_l, \mathcal{M}_l]$. One can then characterize the system trapped at the l th level of the tree by a series of energies $\{\varepsilon_0, \varepsilon_1, \varepsilon_2, \dots, \varepsilon_l\}$ and magnetizations $\{m_0, m_1, m_2, \dots, m_l\}$. The energy and magnetization of the system are given by the sums

$$\begin{aligned} E &= \varepsilon_0 + \varepsilon_1 + \varepsilon_2 + \dots + \varepsilon_l, \\ M &= m_0 + m_1 + m_2 + \dots + m_l. \end{aligned} \quad (2)$$

The characteristic temperatures T_l at different levels are assumed to decrease geometrically with l , i.e., $T_l = T_0 r^l$, where $r < 1$ is a constant. This provides a simple way to encode multiple energy scales into the tree structure while maintaining a finite average total energy $\langle E \rangle = \langle \varepsilon_0 \rangle + \langle \varepsilon_1 \rangle + \langle \varepsilon_2 \rangle + \dots + \langle \varepsilon_l \rangle$ for all l . Consistent with the energy barriers which become smaller with increasing level, we assume the range of magnetization \mathcal{M}_l also decreases geometrically with increasing l .

Following previous works on the hierarchical diffusion models, the relaxation dynamics in a barrier tree is modeled by a random-walk Markov chain process. The transition probability from node α to β is governed by the Metropolis dynamics:

$$P_{\alpha \rightarrow \beta} = Q_{\alpha \rightarrow \beta} \min\{1, e^{-\beta(\mathcal{F}_\beta - \mathcal{F}_\alpha)}\}. \quad (3)$$

Here $\mathcal{F}_\alpha = E_\alpha - HM_\alpha$ is the effective energy of node α , H is a small external probing magnetic field, $\beta \equiv 1/k_B T$ is the inverse temperature, and the coefficient $Q_{\alpha \rightarrow \beta}$ encodes the *structural* information of the tree. As in standard Metropolis dynamics, at every time step, there is a finite probability $P_{\alpha \rightarrow \alpha}$ that the walker stays at the same node; it is determined by the conservation of probability $P_{\alpha \rightarrow \alpha} = 1 - \sum_{\beta \neq \alpha} P_{\alpha \rightarrow \beta}$.

Given a complete representation of the barrier tree, which requires careful labeling of all the nodes at different levels and their connections, the standard Monte Carlo method can be used to simulate the random walk on the barrier. However, although it is possible to explicitly build simple tree structures such as binary trees or single-layer trees, explicit construction of the hierarchical trees with a large number of branching is a computationally demanding task, which requires large runtime memory for storing the tree data. It is also highly inefficient as most of the nodes will not be visited by the walker. To overcome this difficulty, here we develop a dynamical tree method such that new nodes are generated on the fly according to the statistical properties of the tree.

Explicitly, the history of a random walker at level l is kept in two dynamical lists: $\mathcal{L}_\varepsilon = \{\varepsilon_0, \varepsilon_1, \varepsilon_2, \dots, \varepsilon_l\}$ and $\mathcal{L}_m = \{m_0, m_1, m_2, \dots, m_l\}$. These are the energy barrier and magnetization, respectively, of the nodes visited by the walker at each level. If the walker decides to make a down transition to a lower level, random variables ε_{l+1} and m_{l+1} are sampled from their respective probability density and added to the respective history list. On the other hand, the last entries ε_l and m_l are deleted from the respective lists if the walker decides to go up. In doing so, we neglect the possibility that the walker will later visit exactly the same state at the l th level. Nonetheless, this is a reasonable approximation for barrier trees with a large number of branchings, which is usually the case in the thermodynamic limit.

We note that our dynamical tree method is similar to the multilayer random energy model (MREM) used in Refs. [46–48]. The main difference is that their MREM assumes an infinite number of daughters from each node and all nodes except the one at the lowest (outermost) level are saddle points. By excluding local minimum states at intermediate levels, the MREM of [46–48] cannot describe barrier trees of the type shown in Fig. 1(a), which, as will be shown below, exhibits a strong TRM memory effect.

As discussed above, the structure of the barrier tree is encoded in the coefficients $Q_{\alpha \rightarrow \beta}$ in Eq. (3). In our dynamical tree method, these coefficients can also be viewed as a set of transition probabilities that define a separate Markov chain process. Compared with the random walk governed by transition probabilities $P_{\alpha \rightarrow \beta}$, the Markov process corresponding to $Q_{\alpha \rightarrow \beta}$ can be viewed as a random-walk process on the tree *without* the energy constraint. Here we assume these probabilities are given by a few parameters depending on the types of nodes α and β . Explicitly, for a walker stuck in a local minimum α , it can only make a transition to the saddle node β above it. On the other hand, there are three possible transitions that can take place at a saddle point at the l th level: The walker can go to a local minimum of the same level with probability p_0 , jump to a saddle node at the upper level $l - 1$ with probability p_- , or jump to a saddle node at the lower level $l + 1$ with probability p_+ . We summarize these

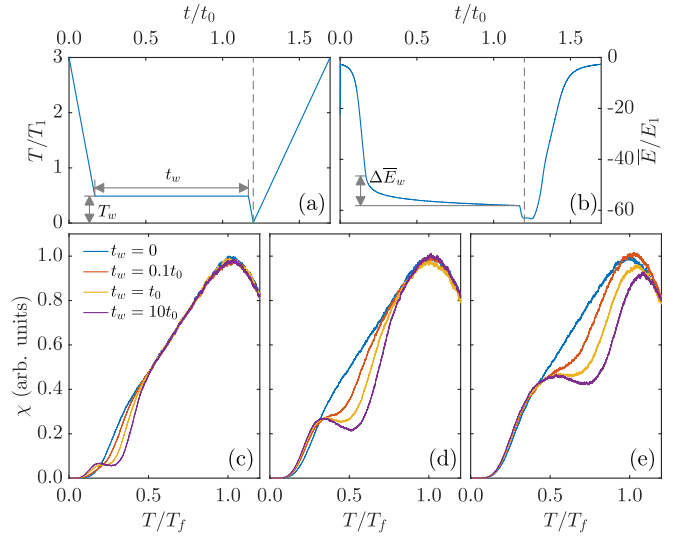


FIG. 2. (a) Protocol for temperature variation for simulating memory effect in multi-layer trap model. The system is initially cooled with a constant rate until the temperature reaches T_w . The system then stays at T_w for a finite period of waiting time t_w before further cooling to a base temperature. During the subsequent measurement, a small magnetic field is applied to induce magnetization while the system is heated with a constant rate. (b) shows the system energy averaged over many independent runs as a function of time. Panels (c)–(e) show the temperature dependence of zero-field-cooled DC magnetic susceptibility χ , generated by Monte Carlo simulations. The data are taken after waiting during the cooling process with the waiting time t_w in units of 5×10^6 Monte Carlo steps at (a) $T_w = 0.2T_f$, (b) $T_w = 0.4T_f$, and (c) $T_w = 0.6T_f$.

transition probabilities as follows:

$$\begin{aligned} Q_{\min \rightarrow \text{saddle}} &= 1, \\ Q_{\text{saddle} \rightarrow \min} &= p_0, \\ Q_{\text{saddle} \rightarrow \text{saddle}} &= p_{\pm}. \end{aligned} \quad (4)$$

Here we have assumed that the probabilities p_0 and p_{\pm} are independent of the levels for simplicity. Physically, the probability p_0 that the system will make a transition from a saddle point α to a local minimum depends on the number of downward pathways from α to one of the minima. For a randomly generated barrier tree with a fixed structure, the number of downward pathways varies from one saddle node to another. Consequently, some saddle node might have more local minima attached to it, hence a larger p_0 . The simplification that these probabilities p_0 and p_{\pm} are constant independent of nodes thus amounts to a mean-field approximation for the tree structure. We note that the introduction of two different probabilities p_{\pm} for moving down and up the backbone tree is similar to the degeneracy factor in, e.g., the binary tree models of Refs. [41–44].

The above dynamical tree generation and the Metropolis random-walk dynamics are used to simulate the TRM memory-dip experiments [18]. The cooling and measurement protocol is summarized in Fig. 2(a). The system is first cooled down from well above T_f to the base temperature with a single stop at an intermediate temperature T_w for some period of time

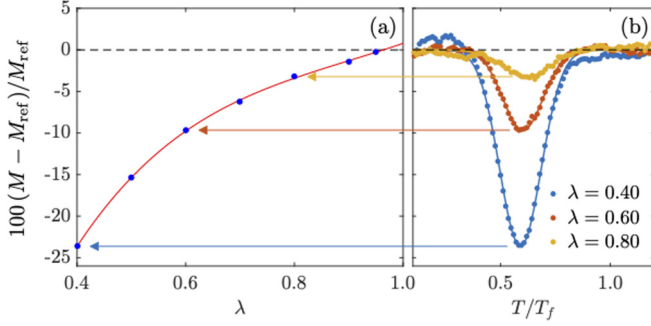


FIG. 3. (a) Memory effect in terms of maximum depth of the relative change of magnetization $(M - M_{\text{ref}})/M_{\text{ref}}$ versus the structural parameter $\lambda = p_+/p_-$. The red line is a guide to the eye. (b) A few examples of the temperature dependence of $(M - M_{\text{ref}})/M_{\text{ref}}$.

t_w under zero field. Once cooled down to the base temperature, the susceptibility $\chi = \langle M \rangle / H$ is measured by applying a small field upon heating at a constant rate. As demonstrated in Figs. 2(c)–2(e), our simulations successfully reproduce the memory effect which manifests as a prominent dip at T_w when the system is heated back. Moreover, the dip becomes more pronounced with increasing waiting time t_w . The sensitive dependence on both waiting temperature T_w and waiting time t_w is the hallmark of the memory effect in thermoremanent magnetization measurement [15–19].

To gain a better insight into this remarkable phenomenon, we plot the average energy $\langle E \rangle$ as a function of time (in terms of Monte Carlo steps) in Fig. 2(b). The energy $\langle E \rangle$ decreases with time initially until the cooling stops at T_w . During this waiting period, the walker cannot efficiently explore those levels l^* whose characteristic energy scales as $T_{l^*} \gtrsim T_w$. This is because the average energy barrier separating nodes at these levels $\varepsilon_B^* \sim T_{l^*}$ is greater than or of similar order to the waiting temperature T_w , hence a small transition probability $P \sim \exp(-T_{l^*}/T_w)$. However, a longer waiting time t_w at T_w allows the walker to overcome the energy barrier ε_B^* through thermal activation and find energetically lower nodes in those levels l^* . This partial equilibration thus gives rise to an additional energy reduction ΔE_w from this waiting period [see Fig. 2(b)]. Upon reheating, again the average energy and level increase with time initially. As the temperature approaches T_w , the system needs to overcome this additional energy barrier ΔE_w , leading to a dip in susceptibility.

Having demonstrated the memory effect in the hierarchical trap model, one natural question is how it is affected by the tree structure. To answer this question, we examine the dependence of the memory effect on a crucial structural parameter

$$\lambda \equiv p_+/p_-, \quad (5)$$

which is the average branching ratio of the backbone tree, i.e., the tree with all local minima removed (see Fig. 1). The backbone tree consists of only the saddle points. Figure 3(a) shows the λ dependence of the relative change of magnetization $(M - M_{\text{ref}})/M_{\text{ref}}$ that provides a quantitative measure of the memory effect, where M and M_{ref} are the magnetization at T_w with and without waiting, respectively [Fig. 3(b)]. Our results show that a pronounced memory effect is obtained with a small λ , corresponding to barrier trees with a smaller

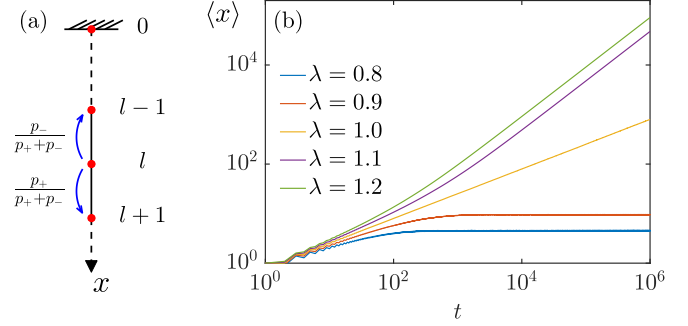


FIG. 4. (a) Schematic diagram of a semi-infinite 1D random walk. In this 1D model, all the saddle nodes at the same level are treated identically, which are represented by red dots. (b) Averaged position $\langle x \rangle$ of the walker as a function of time for different value of $\lambda = p_+/p_-$. Here the average is computed from 10^5 independent Monte Carlo runs.

probability of descending to lower levels. A representative example of such trees is shown in Fig. 1(a).

III. STRUCTURAL PHASE TRANSITION AND CONDENSATION PHENOMENON

Interestingly, the memory effect quickly disappears as λ approaches 1, indicating a potential critical $\lambda_c = 1$. Here we show that this critical point $\lambda_c = 1$ corresponds to the critical point of a structural transition of barrier trees. To this end, we consider a random-walk process which is unaffected by the energy barrier. As discussed above, this Markovian process is governed by the transition probabilities $Q_{\alpha \rightarrow \beta}$, which only depend on the statistical property of the barrier tree. Since a walker at a local minimum will always return to the saddle node according to Eq. (4), we can focus only on the random walk among the saddle nodes, or the backbone tree. The finite probability p_0 that the walker visits the local minima from a given saddle point translates to a finite probability that the walker stays at the same saddle point. The effect of this finite p_0 can then be accounted for by a redefinition of the time step which corresponds to the average time the walker stays at the same saddle node. The Markov chain process described by $Q_{\alpha \rightarrow \beta}$ is now effectively reduced into a random-walk problem along a line. In this mapping, the position x of the walker corresponds to the level l of the tree [see Fig. 4(a)]. At each time step, the walker can move to a lower level with probability $\frac{p_-}{p_+ + p_-}$ or to the upper level with probability $\frac{p_+}{p_+ + p_-}$.

A crucial observation here is that the walker cannot go above level $l = 0$, which means that the random-walk problem has a perfectly reflecting boundary condition at the top. Figure 4(b) shows the time dependence of the average position $\langle x \rangle$ (in units of the level index l) of the walker who is initially at level 0. Our results clearly show two distinct dynamical regimes separated by the critical $\lambda_c = 1$. For small $\lambda < \lambda_c$, the average $\langle x \rangle$ saturates to a finite value in the long-time limit. Physically, this can be understood as a balance between the tendency of the walker to move upward and the reflection at the boundary $l = 0$. As a result of this balance, the walker never wanders too far away from the root. This is consistent with the analytical calculation showing that a walker starting

at position $l \neq 0$ will always visit the root in finite time, i.e., the return probability is 1 [65–67]. On the other hand, for $\lambda > \lambda_c$, the average position $\langle x \rangle$ increases linearly with time, which is expected for a biased random walk without boundary. In the special case of $\lambda = \lambda_c$, corresponding to $p_+ = p_-$, we find that, even in the presence of a reflecting boundary, the walker obeys the well-known time dependence $\langle x \rangle \sim t^{1/2}$ for a symmetric random walk [see Fig. 4(b)].

The two distinct dynamical regimes of the one-dimensional (1D) random walk indicate a *structural* transition of the barrier trees at the critical point $\lambda_c = 1$. The average position $\langle x \rangle$ of the walker provides a measure of the average depth of the hierarchical tree. The above results indicate that trees with $\lambda \geq \lambda_c$ could grow indefinitely in depth in our dynamical tree scheme, which means local minima at deep levels ($l \gg 1$) contribute significantly to the “volume” of the phase space. It is worth noting that, although the hierarchical trees could have an infinite number of levels, our choice of temperature parameters T_l ensures that the average energy is bounded, as discussed above. Moreover, the exponential distribution of barrier energy (1) indicates that local minima at lower levels (larger l) are not necessarily deep in terms of energy.

For barrier trees with $\lambda < \lambda_c$, the fact that the average position $\langle x \rangle$ is finite indicates that such barrier trees are dominated by local minima at shallow levels. This can also be understood from the detailed balance condition that is required for the steady-state random walk. Let \mathcal{N}_l be the average number of saddle nodes at level l ; the detailed balance means $\mathcal{N}_l p_+ = \mathcal{N}_{l+1} p_-$. Consequently, we have $\mathcal{N}_l \sim \mathcal{N}_0 \lambda^l$, which means that the number of saddle nodes decreases geometrically with increasing levels for trees with $\lambda < \lambda_c = 1$; an example of such trees is shown in Fig. 1(a).

Importantly, our simulations in Sec. II show that the subcritical trees with $\lambda < \lambda_c$ exhibit a strong memory effect. The fact that such trees are dominated by local minima at a few shallow levels plays an important role in the emergence of the memory effect and is also related to the so-called condensation phenomenon of glassy systems. To this end, we numerically compute the average participation ratio $Y(T)$, which provides a measure of the glassy behavior. It is essentially the sum of squared Boltzmann probabilities [68,69]

$$Y(T) \equiv \left\langle \sum_{\alpha} W_{\alpha}(T)^2 \right\rangle = \left\langle \frac{1}{Z^2} \sum_{\alpha} e^{-2E_{\alpha}/k_B T} \right\rangle, \quad (6)$$

where the summation is over all local minima α , $Z = \sum_{\alpha} e^{-E_{\alpha}/k_B T}$ is the partition function, and $\langle \dots \rangle$ denotes the average over different realizations of the barrier trees. The participation ratio $Y(T)$ is used to quantitatively characterize the so-called condensation phenomenon, in which a smaller-than-exponential set of microstates dominates the Boltzmann measure. Intuitively, the inverse $1/Y(T)$ gives an estimate of the effective number of configurations that contribute to the partition function. In the case that a large number of microstates contribute equally to the Boltzmann sum, the participation ratio $Y \approx 0$. Condensation happens when the sum is dominated by a few states. The participation ratio can be computed analytically for the random energy model (REM) [70,71], which is similar to a one-layer random trap model. In the thermodynamic limit, the REM exhibits a critical temper-

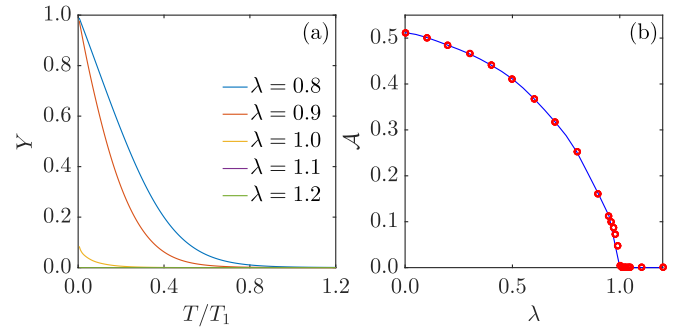


FIG. 5. (a) Participation ratio Y vs temperature for barrier trees obtained from the dynamical tree method. (b) Glassy order parameter \mathcal{A} , defined as the area under the $Y(T)$ curve, vs the tree-structure parameter λ .

ature T_c , above which $Y = 0$. Condensation occurs at $T < T_c$ and the participation ratio grows linearly upon lowering the temperature: $Y(T) \sim 1 - T/T_c$.

Here we perform the Monte Carlo simulation to numerically compute $Y(T)$ for the randomly generated hierarchical trees. It is worth noting that, with our dynamical tree method encoded in transition probabilities $Q_{\alpha \rightarrow \beta}$, the Monte Carlo simulation based on $P_{\alpha \rightarrow \beta}$ automatically provides both the thermal and the disorder average for the calculation of the participation ratio. The numerical temperature dependence of Y is shown in Fig. 5(a) for varying structure factor λ . The behavior of $Y(T)$ here is similar to the REM for $\lambda < 1$. Moreover, the condensation temperature T_c decreases with increasing λ . We can introduce an order parameter

$$\mathcal{A} = \int_0^{\infty} Y(T) dT, \quad (7)$$

which is the area under the $Y(T)$ curve, to characterize the overall degree of condensation or the glassy behavior. Consistent with our random-walk simulation results, the λ dependence of \mathcal{A} indeed shows a critical point at $\lambda_c = 1$, above which the glassy order parameter \mathcal{A} vanishes [see Fig. 5(b)]. The glassy transition at $\lambda_c = 1$ can be viewed as a result of the competition between energy and entropy. While the glassy phase ($\lambda < 1$) is characterized by condensation of a few dominant microstates, the proliferation of energetically shallow minima in trees with $\lambda > 1$ overwhelms those few deep minima, leading to the disappearance of the glassy behavior and memory effect.

IV. CONCLUSION

To summarize, we have numerically demonstrated the memory effect in a dynamical model of hierarchical barrier trees. This numerical simulation successfully shows the nontrivial dependence of the memory effect on the waiting time as well as the waiting temperature. Our results strongly support the crucial role of the hierarchical structure in the memory effect. We further show that trees with a smaller branching ratio, i.e., fewer and fewer saddle points as one goes deeper, tend to exhibit a strong memory effect. In fact, a structural transition of the barrier tree is found to coincide with the glassy transition. This picture is supported by our result

showing that condensation phenomena, in which a few deep local minima dominate the partition function, only occur in trees with a small branching ratio.

We further established a structural transition at the critical point $\lambda_c = 1$, above which the memory effect vanishes. In fact, trees with a large branching ratio $\lambda > \lambda_c$ do not exhibit glassy behavior due to the exponential increase of the number of energetically shallow minima. This picture is supported by our result showing that condensation phenomena, in which a few deep local minima dominate the partition function, only occur in trees with a small branching ratio. The glassy transition at $\lambda_c = 1$ can also be viewed as a result of the competition between energy and entropy. While the glassy phase ($\lambda < 1$) is characterized by condensation of a few dominant microstates, the proliferation of energetically shallow minima in trees with $\lambda > 1$ overwhelms those few deep minima, leading to the disappearance of the glassy behavior and memory effect.

ACKNOWLEDGMENTS

We are grateful for valuable discussions with P. Charbonneau, I. Klich, and L. F. Cugliandolo. D.Z. and S.-H.L. acknowledge support from the U.S. Department of Energy (DOE), Office of Science, Basic Energy Sciences under Award No. DE-SC0016144. M.V. was supported by the National Science Foundation under Grant No. DMR-1944539. G.-W.C. was partially supported by the Center for Materials Theory as a part of the Computational Materials Science program, funded by the DOE Office of Science, Basic Energy Sciences, Materials Sciences and Engineering Division. The authors also acknowledge the support of Research Computing at the University of Virginia.

APPENDIX A: DYNAMICAL TREE METHOD

In the Appendixes we provide the pseudocodes for the algorithms used in this work, including the dynamical tree methods for the thermoremanent magnetization simulation, the 1D random-walk simulation, and the participation ratio simulation. Details of the simulations are also discussed.

In order to avoid the extremely large memory to precreate the entire tree, we generate the tree nodes on the fly. In the dynamical tree method, only the node level l and the lists of barrier energies and magnetizations, i.e., \mathcal{L}_ε and \mathcal{L}_m , respectively, are kept tracked of during the simulation. An additional parameter is_min is used to label whether the current node is a local minimum or a saddle point. The simulations are performed on a temperature series Ts along with a magnetic field series Hs . At each temperature point, the total magnetic moment is averaged over n_{sweep} iterations and recorded in a list Ms . In each iteration, the system can choose to walk up, $l \rightarrow l - 1$, or down, $l \rightarrow l + 1$, based on the node condition and the Metropolis-Hastings algorithm. See Algorithm 1 for details.

The parameters we used to produce Fig. 2 in the main text are the total number of tree levels $L = 100$ and the branching number at each saddle point, $N_b = 20$; both the characteristic energy T_l and characteristic magnetization \mathcal{M}_l follow geometric distributions, i.e., $T_l = T_0 r^l$ and $\mathcal{M}_l = \mathcal{M}_0 r^l$, where

Algorithm 1 Dynamical Tree Method

```

 $l \leftarrow 0$  ▷ start from root at level 0
 $is\_min \leftarrow false$  ▷ label local minimum
 $\mathcal{L}_\varepsilon \leftarrow [0] \times (L + 1)$  ▷ keep record of  $\varepsilon_l$ 
 $\mathcal{L}_m \leftarrow [0] \times (L + 1)$  ▷ keep record of  $m_l$ 
 $Ms \leftarrow [0] \times len(Ts)$  ▷ magnetic moment

for  $i$  in  $0 \dots len(Ts) - 1$  do
   $T \leftarrow Ts[i]$  ▷ temperature
   $H \leftarrow Hs[i]$  ▷ magnetic field
  for  $j$  in  $0 \dots n_{sweep} - 1$  do
    if  $l = 0$  or  $is\_min = false$  and  $rand() > \frac{1}{1+N_b}$  then
      ▷ go down if at level 0 or saddle point ( $rand() > \frac{1}{1+N_b}$ )
       $\varepsilon_l \leftarrow -T_l \log(rand())$ 
       $m_l \leftarrow \mathcal{M}_l(2 \cdot rand() - 1)$ 
       $\Delta \mathcal{E} \leftarrow -\varepsilon_l - Hm_l$ 
      if  $rand() < e^{-\Delta \mathcal{E}/T}$  then
         $\mathcal{L}_\varepsilon[l] \leftarrow \varepsilon_l$ 
         $\mathcal{L}_m[l] \leftarrow m_l$ 
         $is\_min \leftarrow rand() > \frac{\lambda}{N_b}$ 
         $l \leftarrow l + 1$ 
      end if
    else
      ▷ go up if at minimum or saddle point ( $rand() < \frac{1}{1+N_b}$ )
       $\varepsilon_{l-1} \leftarrow \mathcal{L}_\varepsilon[l - 1]$ 
       $m_{l-1} \leftarrow \mathcal{L}_m[l - 1]$ 
       $\Delta \mathcal{E} \leftarrow \varepsilon_{l-1} + Hm_{l-1}$ 
      if  $rand() < e^{-\Delta \mathcal{E}/T}$  then
         $\mathcal{L}_\varepsilon[l - 1] \leftarrow 0$ 
         $\mathcal{L}_m[l - 1] \leftarrow 0$ 
         $l \leftarrow l - 1$ 
      end if
    end if
  end for
   $M \leftarrow sum(\mathcal{L}_m)$  ▷ total magnetic moment
   $Ms[i] \leftarrow \frac{i * Ms[i] + M}{i + 1}$  ▷ keep running average
end for

```

$T_0 = 1$, $\mathcal{M}_0 = 0.5$, and $r = 0.97$; the parameter λ is also level dependent, $\lambda = \frac{1-p^{L-1-l}}{N_b}$, where $p = 0.9998$.

Based on the thermoremanent magnetization experiments, the temperature and magnetic field series Ts and Ms , respectively, are set to be four processes: (i) zero-field cooling,

Algorithm 2 1D Random Walk

```

 $l \leftarrow 0$  ▷ start from root at level 0
 $Ls \leftarrow [0] \times (t + 1)$  ▷ keep record of walker's level

for  $i$  in  $1 \dots t$  do
  ▷ go down if at level 0 or  $rand() < \frac{\lambda}{\lambda + 1}$ , go down otherwise
  if  $l = 0$  or  $rand() < \frac{\lambda}{\lambda + 1}$  then
     $l \leftarrow l + 1$ 
  else
     $l \leftarrow l - 1$ 
  end if
   $Ls[i] \leftarrow l$ 
end for

```

Algorithm 3 Participation Ratio Simulation

```

 $l \leftarrow 0$  ▷ start from root at level 0
 $is\_min \leftarrow false$  ▷ label local minimum
 $\mathcal{L}_\varepsilon \leftarrow [0] \times (L + 1)$  ▷ keep record of  $\varepsilon_l$ 
 $B1s = [0] \times len(Ts)$ 
 $B2s = [0] \times len(Ts)$ 
 $PRs = [0] \times len(Ts)$  ▷ keep record of PR

for  $i$  in  $0 \dots n_{wait} + n_{count} - 1$  do
  if  $l = 0$  or  $is\_min = false$  and  $rand() > \frac{1}{1+N_b}$  then
    ▷ go down if at level 0 or saddle point ( $rand() > \frac{1}{1+N_b}$ )
    if  $rand() < \frac{\lambda}{N_b}$  then
       $\mathcal{L}_\varepsilon[l] \leftarrow T_l \log(rand())$ 
       $l \leftarrow l + 1$ 
    else
       $is\_min \leftarrow true$ 
    end if
  else
    ▷ go up if at minimum or saddle point ( $rand() < \frac{1}{1+N_b}$ )
    if  $is\_min = true$  then
       $is\_min \leftarrow false$ 
    else
       $\mathcal{L}_\varepsilon[l - 1] \leftarrow 0$ 
       $l \leftarrow l - 1$ 
    end if
  end if
end if

if  $i > n_{wait}$  and  $is\_min = true$  then
  ▷ count at minimum after waiting
   $T \leftarrow Ts[j]$ 
   $E \leftarrow sum(\mathcal{L}_\varepsilon) + T_l \log(rand())$ 
  for  $j$  in  $0 \dots len(Ts) - 1$  do
     $B1s[j] \leftarrow B1s[j] + e^{-E/T}$ 
     $B2s[j] \leftarrow B2s[j] + e^{-2E/T}$ 
     $PRs[j] \leftarrow \frac{B2s[j]}{B1s[j]^2}$ 
  end for
end if
end for

```

with no magnetic field $H = 0$ and a linearly decreasing temperature from $T = T_{\max}$ to $T = T_w$ in $\frac{T_{\max} - T_w}{T_{\max} - T_{\min}} N_c$ steps; (ii) zero-field waiting, with $H = 0$ and $T = T_w$ in N_w steps;

(iii) zero-field cooling, with $H = 0$ and from $T = T_w$ to $T = T_{\min}$ in $\frac{T_w - T_{\min}}{T_{\max} - T_{\min}} N_c$ steps; and (iv) field reheating, with $H = 1$ and from $T = T_{\min}$ to $T = T_{\max}$ in N_h linear steps, where the minimum temperature is $T_{\min} = 0.01$, the maximum temperature is $T_{\max} = 3.00$, the waiting temperature is $T_w = 0.2T_f, 0.4T_f, 0.6T_f$ ($T_f \approx 1.22$), the total number of cooling steps is $N_c = 2 \times 10^4$, the number of heating steps is $N_c = 5 \times 10^4$, the number of waiting steps is $N_c = 0, 10^3, 10^4, 10^5, 10^6$, and the iteration number at each temperature point is $n_{\text{sweep}} = 50$. In addition to the thermal average, the final temperature-dependent magnetization and susceptibility are averaged over $n_{\text{sample}} = 10^5$ simulations.

In order to simulate the λ dependence in Fig. 3 in the main text, we changed the λ parameter to a level-independent uniform value, and the total tree level is extended from $L = 100$ to $L = 200$. Furthermore, T_{\max} is changed to accommodate the different T_f values, i.e., $T_{\max} = 1.2T_f$, where $T_f \approx 1.24, 1.40, 1.59, 1.87, 2.37, 3.54, 5.16$ for $\lambda = 0.4, 0.5, 0.6, 0.7, 0.8, 0.9, 0.95$, and the waiting temperature is set at $T_w = 0.5T_{\max}$.

APPENDIX B: 1D RANDOM WALK

As is discussed in the main text, to map the dynamical tree method to a 1D random walk, the probability to move to a lower level and a high level from $l > 0$ should be $\frac{p_+}{p_+ + p_-} = \frac{\lambda}{\lambda + 1}$ and $\frac{p_-}{p_+ + p_-} = \frac{1}{\lambda + 1}$. The algorithm for the 1D random-walk simulation is shown in Algorithm 2, where the parameter λ is chosen to be 0.8–1.2. In addition, the results were taken for $t = 10^6$ steps and averaged over $n_{\text{sample}} = 10^5$ samples.

APPENDIX C: PARTICIPATION RATIO SIMULATION

The algorithm for the participation ratio simulation is shown in Algorithm 3, which is the $T \rightarrow 0$ limit of the dynamical tree method. The parameters used are the geometrically distributed characteristic energy $T_l = T_0 r^l$, where $T_0 = 1$, $r = 0.95$, the branching number $N_b = 100$, and $\lambda = 0.00\text{--}1.20$. The participation ratios are calculated based on a linear temperature series $Ts = \{0.005, 0.010, 0.015, \dots, 1.995, 2.000\}$ and averaged over $n_{\text{sample}} = 10^4$ samples and over $n_{\text{count}} = 10^6$ iterations after thermal equilibrium in $n_{\text{wait}} = 10^6$ walking steps.

[1] E. Vincent, J. Hammann, M. Ocio, J.-P. Bouchaud, and L. F. Cugliandolo, in *Complex Behavior of Glassy Systems*, edited by M. Rubi, Lecture Notes in Physics (Springer, Berlin, 1997), Vol. 492, pp. 184–219.

[2] J.-P. Bouchaud, L. F. Cugliandolo, J. Kurchan, and M. Mézard, in *Spin-Glass and Random Fields*, edited by A. P. Young (World Scientific, Singapore, 1998), pp. 161–224.

[3] *Ageing and the Glass Transition*, edited by M. Henkel, M. Pleimling, and R. Sanctuary, Lecture Notes in Physics Vol. 716 (Springer, Berlin, 2007).

[4] M. Henkel and M. Pleimling, *Non-Equilibrium Phase Transitions* (Springer, Berlin, 2010), Vol. 2.

[5] For a review see, e.g., V. Dupuis, F. Bert, J.-P. Bouchaud, J. Hammann, F. Ladieu, D. Parker, and E. Vincent, Aging, rejuvenation, memory phenomena in spin glasses, *Pramana* **64**, 1109 (2005).

[6] E. Vicent and V. Dupuis, in *Frustrated Materials and Ferroic Glasses*, edited by T. Lookman and X. Ren, Springer Series in Material Science (Springer, Berlin, 2018), Vol. 275, pp. 31–56.

[7] P. Svedlindh, P. Granberg, P. Nordblad, L. Lundgren, and H. S. Chen, Relaxation in spin glasses at weak magnetic fields, *Phys. Rev. B* **35**, 268 (1987).

[8] P. Granberg, L. Sandlund, P. Nordblad, P. Svedlindh, and L. Lundgren, Observation of a time-dependent spatial correlation length in a metallic spin glass, *Phys. Rev. B* **38**, 7097 (1988).

- [9] F. Lefloch, J. Hammann, M. Ocio, and E. Vincent, Can aging phenomena discriminate between the droplet model and a hierarchical description in spin glasses? *Europhys. Lett.* **18**, 647 (1992).
- [10] J. O. Andersson, J. Mattsson, and P. Nordblad, Overlap length in a Cu-Mn spin glass probed by ac susceptibility, *Phys. Rev. B* **48**, 13977 (1993).
- [11] K. Jonason, E. Vincent, J. Hammann, J. P. Bouchaud, and P. Nordblad, Memory and Chaos Effects in Spin Glasses, *Phys. Rev. Lett.* **81**, 3243 (1998).
- [12] L. W. Bernardi, H. Yoshino, K. Hukushima, H. Takayama, A. Tobo, and A. Ito, Aging of the Zero-Field-Cooled Magnetization in Ising Spin Glasses: Experiment and Numerical Simulation, *Phys. Rev. Lett.* **86**, 720 (2001).
- [13] R. Mathieu, P. E. Jönsson, P. Nordblad, H. Aruga Katori, and A. Ito, Memory and chaos in an ising spin glass, *Phys. Rev. B* **65**, 012411 (2001).
- [14] R. Mathieu, M. Hudl, and P. Nordblad, Memory and rejuvenation in a spin glass, *Europhys. Lett.* **90**, 67003 (2010).
- [15] H. Mamiya and S. Nimori, Memory effects in Heisenberg spin glasses: Spontaneous restoration of the original spin configuration rather than preservation in a frozen state, *J. Appl. Phys.* **111**, 07E147 (2012).
- [16] H. Mamiya, N. Tsujii, N. Terada, S. Nimori, H. Kitazawa, A. Hoshikawa, and T. Ishigaki, Slow dynamics in the geometrically frustrated magnet ZnFe_2O_4 : Universal features of aging phenomena in spin glasses, *Phys. Rev. B* **90**, 014440 (2014).
- [17] H. Mamiya, Universal memory effects in Heisenberg spin glasses and spontaneous restoration of the spin configuration, *Phys. Proc.* **75**, 711 (2015).
- [18] A. Samarakoon, T. J. Sato, T. Chen, G.-W. Chern, J. Yang, I. Klich, R. Sinclair, H. Zhou, and S.-H. Lee, Aging, memory, and nonhierarchical energy landscape of spin jam, *Proc. Natl. Acad. Sci. USA* **113**, 11806 (2016).
- [19] A. M. Samarakoon, M. Takahashi, D. Zhang, J. Yang, N. Katayama, R. Sinclair, H. D. Zhou, S. O. Diallo, G. Ehlers, D. A. Tennant, S. Wakimoto, K. Yamada, G.-W. Chern, T. J. Sato, and S.-H. Lee, Scaling of memories and crossover in glassy magnets, *Sci. Rep.* **7**, 12053 (2017).
- [20] J.-P. Bouchaud, V. Dupuis, J. Hammann, and E. Vincent, Separation of time and length scales in spin glasses: Temperature as a microscope, *Phys. Rev. B* **65**, 024439 (2001).
- [21] Y. G. Joh, R. Orbach, G. G. Wood, J. Hammann, and E. Vincent, Extraction of the Spin Glass Correlation Length, *Phys. Rev. Lett.* **82**, 438 (1999).
- [22] D. A. Huse, Monte Carlo simulation study of domain growth in an Ising spin glass, *Phys. Rev. B* **43**, 8673 (1991).
- [23] E. Marinari, G. Parisi, F. Ritort, and J. J. Ruiz-Lorenzo, Numerical Evidence for Spontaneously Broken Replica Symmetry in 3D Spin Glasses, *Phys. Rev. Lett.* **76**, 843 (1996).
- [24] T. Komori, H. Yoshino, and H. Takayama, Numerical study on aging dynamics in the 3D Ising spin-glass model. I. Energy relaxation and domain coarsening, *J. Phys. Soc. Jpn.* **68**, 3387 (1999).
- [25] D. S. Fisher and D. A. Huse, Nonequilibrium dynamics of spin glasses, *Phys. Rev. B* **38**, 373 (1988).
- [26] G. J. M. Koper and H. J. Hilhorst, A domain theory for linear and nonlinear aging effects in spin glasses, *J. Phys. (Paris)* **49**, 429 (1988).
- [27] H. Yoshino, A. Lemaître, and J.-P. Bouchaud, Multiple domain growth and memory in the droplet model for spin-glasses, *Eur. Phys. J. B* **20**, 367 (2001).
- [28] M. Baity-Jesi, R. A. Baños, A. Cruz, L. A. Fernandez, J. M. Gil-Narvion, A. Gordillo-Guerrero, D. Iñiguez, A. Maiorano, F. Mantovani, E. Marinari, V. Martin-Mayor, J. Monforte-Garcia, A. Muñoz Sudupe, D. Navarro, G. Parisi, S. Perez-Gaviro, M. Pivanti, F. Ricci-Tersenghi, J. J. Ruiz-Lorenzo, S. F. Schifano, B. Seoane, A. Tarancon, R. Tripiccion, and D. Yllanes (Janus Collaboration), Temperature chaos is present in off-equilibrium spin-glass dynamics, *Commun. Phys.* **4**, 74 (2021).
- [29] M. Picco, F. Ricci-Tersenghi, and F. Ritort, Chaotic, memory, and cooling rate effects in spin glasses: Evaluation of the Edwards-Anderson model, *Phys. Rev. B* **63**, 174412 (2001).
- [30] P. E. Jönsson, R. Mathieu, P. Nordblad, H. Yoshino, H. Aruga Katori, and A. Ito, Nonequilibrium dynamics of spin glasses: Examination of the ghost domain scenario, *Phys. Rev. B* **70**, 174402 (2004).
- [31] S. Jiménez, V. Martín-Mayor, and S. Pérez-Gaviro, Rejuvenation and memory in model spin glasses in three and four dimensions, *Phys. Rev. B* **72**, 054417 (2005).
- [32] M. Baity-Jesi, R. A. Baños, A. Cruz, L. A. Fernandez, J. M. Gil-Narvion, A. Gordillo-Guerrero, D. Iñiguez, A. Maiorano, F. Mantovani, E. Marinari, V. Martin-Mayor, J. Monforte-Garcia, A. Muñoz Sudupe, D. Navarro, G. Parisi, S. Perez-Gaviro, M. Pivanti, F. Ricci-Tersenghi, J. J. Ruiz-Lorenzo, S. F. Schifano, B. Seoane, A. Tarancon, R. Tripiccion, and D. Yllanes (Janus Collaboration), Dynamical transition in the $D = 3$ Edwards-Anderson spin glass in an external magnetic field, *Phys. Rev. E* **89**, 032140 (2014).
- [33] P. Sibani and S. Boettcher, Mesoscopic real-space structures in spin-glass aging: The Edwards-Anderson model, *Phys. Rev. B* **98**, 054202 (2018).
- [34] B. Derrida, Random-Energy Model: Limit of a Family of Disordered Models, *Phys. Rev. Lett.* **45**, 79 (1980).
- [35] J. P. Bouchaud, Weak ergodicity breaking and aging in disordered systems, *J. Phys. I (Paris)* **2**, 1705 (1992).
- [36] K. H. Hoffmann, A. Fischer, S. Schubert, and T. Streibert, in *Parallel Algorithms and Cluster Computing*, edited by K. H. Hoffman and A. Meyer, Lecture Notes in Computer Science and Engineering (Springer, Berlin, 2006), pp. 281–302.
- [37] G. Paladin, M. Mézard, and C. de Dominicis, Diffusion in an ultrametric space: A simple case, *J. Phys. (Paris) Lett.* **46**, L985 (1985).
- [38] A. T. Ogielski and D. L. Stein, Dynamics on Ultrametric Spaces, *Phys. Rev. Lett.* **55**, 1634 (1985).
- [39] P. Sibani, Anomalous diffusion and low-temperature spin-glass susceptibility, *Phys. Rev. B* **35**, 8572 (1987).
- [40] J. C. Dyre, Master-Equation Approach to the Glass Transition, *Phys. Rev. Lett.* **58**, 792 (1987).
- [41] K. H. Hoffmann and P. Sibani, Diffusion in hierarchies, *Phys. Rev. A* **38**, 4261 (1988).
- [42] P. Sibani and K. H. Hoffmann, Hierarchical Models for Aging and Relaxation of Spin Glasses, *Phys. Rev. Lett.* **63**, 2853 (1989).
- [43] C. Schulze, K. H. Hoffmann, and P. Sibani, Aging phenomena in complex systems: A hierarchical model for temperature step experiments, *Europhys. Lett.* **15**, 361 (1991).

- [44] K. H. Hoffmann, S. Schubert, and P. Sibani, Age reinitialization in hierarchical relaxation models for spin-glass dynamics, *Europhys. Lett.* **38**, 613 (1997).
- [45] H. Yoshino, Hierarchical diffusion, aging and multifractality, *J. Phys. A: Math. Gen.* **30**, 1143 (1997).
- [46] M. Sasaki and K. Nemoto, Aging phenomena of magnetization in a hierarchical diffusion model, *J. Phys. Soc. Jpn.* **68**, 1148 (1999).
- [47] M. Sasaki and K. Nemoto, Memory effect, rejuvenation and chaos effect in the multi-layer random energy model, *J. Phys. Soc. Jpn.* **69**, 2283 (2000).
- [48] M. Sasaki and K. Nemoto, Analysis on aging in the generalized random energy model, *J. Phys. Soc. Jpn.* **69**, 3045 (2000).
- [49] G. B. Arous, A. Bovier, and V. Gayrard, Aging in the Random Energy Model, *Phys. Rev. Lett.* **88**, 087201 (2002).
- [50] P. Moretti, A. Baronchelli, A. Barrat, and R. Pastor-Satorras, Complex networks and glassy dynamics: Walks in the energy landscape, *J. Stat. Mech.* (2011) P03032.
- [51] M. Baity-Jesi, G. Biroli, and C. Cammarota, Activated aging dynamics and effective trap model description in the random energy model, *J. Stat. Mech.* (2018) 013301.
- [52] P. Sibani, J. C. Schön, P. Salamon, and J.-O. Andersson, Emergent hierarchical structures in complex-system dynamics, *Europhys. Lett.* **22**, 479 (1993).
- [53] M. Lederman, R. Orbach, J. M. Hammann, M. Ocio, and E. Vincent, Dynamics in spin glasses, *Phys. Rev. B* **44**, 7403 (1991).
- [54] E. Vincent, J. Hammann, and M. Ocio, Real spin glasses relax slowly in the shade of hierarchical trees, *J. Stat. Phys.* **135**, 1105 (2009).
- [55] Z. Ling-Nan and S. R. Nagel, Glassy Dynamics in Thermally Activated List Sorting, *Phys. Rev. Lett.* **104**, 257201 (2010).
- [56] P. Garstecki, T. X. Hoang, and M. Cieplak, Energy landscapes, supergraphs, and “folding funnels” in spin systems, *Phys. Rev. E* **60**, 3219 (1999).
- [57] W. Hordijk, J. F. Fontanari, and P. F. Stadler, Shapes of tree representations of spin-glass landscapes, *J. Phys. A: Math. Gen.* **36**, 3671 (2003).
- [58] D. J. Wales and J. P. K. Doye, Dynamics and thermodynamics of supercooled liquids and glasses from a model energy landscape, *Phys. Rev. B* **63**, 214204 (2001).
- [59] F. Despa, D. J. Wales, and R. S. Berry, Archetypal energy landscapes: Dynamical diagnosis, *J. Chem. Phys.* **122**, 024103 (2005).
- [60] D. J. Wales, *Energy Landscapes* (Cambridge University Press, Cambridge, 2003).
- [61] O. M. Becker and M. Karplus, The topology of multidimensional potential energy surfaces: Theory and application to peptide structure and kinetics, *J. Chem. Phys.* **106**, 1495 (1997).
- [62] D. J. Wales, M. A. Miller, and T. R. Walsh, Archetypal energy landscapes, *Nature (London)* **394**, 758 (1998).
- [63] Q. Zhou and W. H. Wong, Energy landscape of a spin-glass model: Exploration and characterization, *Phys. Rev. E* **79**, 051117 (2009).
- [64] S. De, B. Schaefer, A. Sadeghi, M. Sicher, D. G. Kanhere, and S. Goedecker, Relation between the Dynamics of Glassy Clusters and Characteristic Features of their Energy Landscape, *Phys. Rev. Lett.* **112**, 083401 (2014).
- [65] M. Wright, Boundary problems for one and two dimensional random walks, M.S. thesis, Western Kentucky University, 2015.
- [66] M. Khantha and V. Balakrishnan, Reflection principles for biased random walks and application to escape time distributions, *J. Stat. Phys.* **41**, 811 (1985).
- [67] S. R. Finch, How far might we walk at random? [arXiv:1802.04615](https://arxiv.org/abs/1802.04615).
- [68] D. Gross and M. Mézard, The simplest spin glass, *Nucl. Phys. B* **240**, 431 (1984).
- [69] M. Mézard and A. Montanari, *Information, Physics, and Computation* (Oxford University Press, Oxford, 2009).
- [70] M. Mézard, G. Parisi, and M. A. Virasoro, Random free energies in spin glasses, *J. Phys. (Paris) Lett.* **46**, L217 (1985).
- [71] B. Derrida and G. Toulouse, Sample to sample fluctuations in the random energy model, *J. Phys. (Paris) Lett.* **46**, L223 (1985).